JACS
JOURNAL OF THE AMERICAN CHEMICAL SOCIETY
Article
pubs.acs.org/JACS

Synthesis, Structures, and Solution Dynamics of Tetrasubstituted Nine-Atom Germanium Deltahedral Clusters

Feng Li and Slavi C. Sevov*

Department of Chemistry and Biochemistry, University of Notre Dame, Notre Dame, Indiana 46556, United States

Supporting Information

ABSTRACT: Reported are the rational synthesis, structures, and solution dynamics of three tetrasubstituted and neutral Ge_9-based deltahedral clusters $[Ge_9R_3R']^0$, where R = $Si(SiMe_3)_3$ and R′ = Et (**1**), Sn^nBu_3 (**2**), or Tl (**3**). The first step of the synthesis is a reaction of an acetonitrile suspension of the intermetallic precursor compound K_4Ge_9 with $\{Si(SiMe_3)_3\}Cl$ which produces the trisubstituted monoanions $[Ge_9\{Si(SiMe_3)_3\}]^-$. A benzene suspension of the latter is then reacted with Sn^nBu_3Cl or TlCp to produce **2** and **3**, respectively, while the same acetonitrile solution is reacted with EtBr in order to produce **1**. All three structures can be viewed as tricapped trigonal prisms of Ge_9 with the three "hypersilyl" substituents, $Si(SiMe_3)_3$, *exo*-bonded to the capping atoms. The fourth substituent in **1**, the ethyl group, is *exo*-bonded to one of the six available Ge atoms with the Ge−C bond positioned radially to the Ge_9 core. In the case of **2**, on the other hand, the tin fragment is found above one of the triangular bases of the prism interacting with one or more Ge atoms in three crystallographically different molecules in the structure. Lastly, the Tl atom in the structure of **3** is found capping a pseudosquare face between two hypersilyl substituents. NMR spectroscopy indicates that all three compounds are dynamic at room temperature. Variable-temperature studies suggest that the process in **1** and **2** is intramolecular while the process in **3** involves dissociation of the Tl^+ ion from the molecule followed by association at the same or another equivalent pseudosquare face of the molecule. Thus, the latter compound may be considered to a large extent to be ionic as it is made of a thallium cation and a trisubstituted cluster anion.

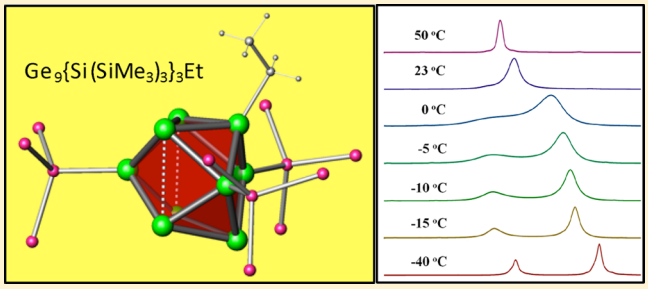

INTRODUCTION

The functionalization of nine-atom deltahedral Zintl anions of germanium with various substituents has become a fairly rich field of cluster chemistry in recent years.[1] The subfield of functionalization with organic and main-group organometallic fragments is a major part of this chemistry.[2−10] However, for more than a decade, the only known such functionalized species were with one or two substituents, such as $[Ge_9R]^{3-}$ and $[Ge_9R_2]^{2-}$, respectively. This status quo held until recently when we reported the rational synthesis of tri- and tetrasubstituted species $[Ge_9R_3]^-$ and $[Ge_9R_3R']^0$, respectively, where R = $-Si(SiMe_3)_3$ and R′ = $-SnPh_3$.[11,12] The breakthrough was achieved by exploring the reactivity of the clusters in somewhat atypical solvents for this chemistry. While the common solvents for these reactions, ethylenediamine and liquid ammonia, are excellent media for attaching one and two substituents, they were inappropriate, for one reason or another, when trying to add three and four substituents. Historically, they have been the solvents of choice in the Zintl ion chemistry for the simple reason that they are the best solvents for dissolving the starting intermetallic precursors, and the resulting solutions are stable for long time; that is, the solvent is not reduced by the clusters. Our approach was to test solvents that do not necessarily dissolve the precursor but would dissolve the eventual products of tri- and tetrasubstituted clusters. Thus, the reaction of a suspension of K_4Ge_9 in either acetonitrile or THF (slower reaction compared to acetonitrile) with $(SiMe_3)_3SiCl$ produced almost exclusively and quantitatively the trisubstituted monoanion $[Ge_9(Si(SiMe_3)_3)_3]^-$, which has excellent solubility in both solvents.[11] Furthermore, applying the same approach to the latter monoanion by making a suspension/solution of it in benzene (the compound is moderately soluble) and reacting it with Ph_3SnCl led to the already reported tetrasubstituted and neutral molecule $[Ge_9\{Si(SiMe_3)_3\}_3\{SnPh_3\}]^0$ (**4**).[12]

We point out that, originally, the monoanion $[Ge_9(Si(SiMe_3)_3)_3]^-$ was synthesized in low yields without using preassembled Ge_9 deltahedral clusters but rather by reacting metastable GeBr with LiR at low temperature.[13] Furthermore, various transition-metal fragments have been added to the monoanion to form $[Ge_9R_3M(CO)_x]^-$ (x = 3 or 5, M = Cr, Mo, and W)[14,15] and $[Ge_9R_3MGe_9R_3]^{n-}$ (n = 1 for M = Cu, Ag, and Au; n = 0 for M = Zn, Cd, and Hg).[16−18]

Herein, we report the synthesis of three more neutral molecules with Ge_9 deltahedral cores, namely, $[Ge_9R_3Et]$ (**1**), $[Ge_9R_3Sn^nBu_3]$ (**2**), and $[Ge_9R_3Tl]$ (**3**), where R = $-Si(SiMe_3)_3$, referred to as "hypersilyl" throughout the text. We

Received: June 10, 2014
Published: August 12, 2014

   dx.doi.org/10.1021/ja505826x | J. Am. Chem. Soc. 2014, 136, 12056−12063

also present results from our studies on the dynamics of the substituents observed in all known tetrasubstituted Ge_9 clusters so far. We point out that compound **1** represents the first neutral tetrasubstituted Ge_9 cluster with an organic substituent.

EXPERIMENTAL SECTION

Materials and Synthesis. All manipulations were carried out under nitrogen atmosphere in a glovebox. The Zintl phase precursor K_4Ge_9 was synthesized from a stoichiometric mixture of the elements (K, Aldrich, 99.5%; Ge, Alfa-Aesar, 99.999%) heated at 950 °C over 2 days in sealed niobium containers jacketed in evacuated fused silica tubes. Hexanes (Alfa-Aesar, 98.5+%) and toluene (Alfa-Aesar, anhydrous, 99.8+%) were dried by passing over copper-based catalyst and 4 Å molecular sieves and were then stored in gastight ampules under nitrogen. Acetonitrile (EMD-DriSolv, anhydrous, 99.8+%) and benzene (Alfa-Aesar, anhydrous, 99.8+%) were stored over molecular sieves in gastight ampules under nitrogen. Hypersilyl chloride $(Me_3Si)_3SiCl$ (chlorotris(trimethylsilyl)silane, TCI, 95+%), $^nBu_3SnCl$ (tri-*n*-butyltin chloride, Alfa-Aesar, 96%), TlCp (cyclopentadienylthallium, Strem Chemicals, 95%), EtBr (bromoethane, Alfa-Aesar, 98+%), and *n*-BuBr (1-bromobutane, TCI, 98+%) were used as received.

Synthesis of $[Ge_9\{Si(SiMe_3)_3\}_3Et]$ (1). K_4Ge_9 (92 mg, 0.114 mmol) was weighed out in a test tube in the glovebox, and acetonitrile (3.0 mL) solution of $(Me_3Si)_3SiCl$ (101 mg, 0.356 mmol) was added to the test tube. The reaction mixture was stirred for 4 h at room temperature and then filtered. EtBr (61 mg, 0.560 mmol) in 0.5 mL of acetonitrile was added to the clear red solution dropwise while stirring, and yellow-brown precipitate started to form in 15 min. After 4 h of stirring, the solution became almost colorless while the color of the precipitate changed somewhat to more brownish. This precipitate was washed with acetonitrile three times and was redissolved in toluene to give a dark red solution. After any undissolved solid was separated by a centrifuge, the dark red solution was concentrated under vacuum and then stored at −20 °C for crystallization. Large red block-like crystals suitable for single-crystal X-ray crystallography were obtained after 1 week (ca. 70% yield). ^{1}H NMR (23 °C, toluene-d_8): δ 1.779 (q, CH_2), 1.446 (tri, CH_3 on the ethyl), 0.387 (s, broad, CH_3 on the hypersilyl). ^{13}C NMR (23 °C, toluene-d_8): δ 21.992 (CH_3 on the ethyl), 4.285 (CH_2 on the ethyl), 2.687 (CH_3 on the hypersilyl). ^{29}Si NMR (23 °C, toluene-d_8): δ −8.019 ($SiMe_3$), −105.879 (Si).

Crystallization of $[Ge_9\{Si(SiMe_3)_3\}_3\{Sn^nBu_3\}]$ (2). This compound was prepared following the procedure described in ref 12 but using $^nBu_3SnCl$ instead of Ph_3SnCl. After the benzene solvent was removed from the final solution, the resulting solid was redissolved in toluene. After concentration under vacuum, the solution was stored at −20 °C for crystallization. Large, dark black-red, needle-like single crystals suitable for X-ray crystallography were obtained after several weeks (ca. 80% yield).

Synthesis of $[Ge_9Tl\{Si(SiMe_3)_3\}_3]$ (3). K_4Ge_9 (121 mg, 0.149 mmol) was weighed out in a test tube in the glovebox, and acetonitrile (3.0 mL) solution of $(Me_3Si)_3SiCl$ (136 mg, 0.379 mmol) was added to the test tube. The reaction mixture was stirred for 4 h at room temperature and filtered, and the solvent was removed under vacuum. Benzene (3.0 mL) suspension of TlCp (106 mg, 0.393 mmol) was added to extract the red solid residue and formed a dark red suspension initially. This reaction mixture was stirred for another 4 h during which the suspension became a darker brick-reddish solution. The solution was filtered, and the benzene solvent was removed under vacuum. Toluene was added to extract the brick-red solid residue. After concentration under vacuum, the solution was stored at −20 °C for crystallization. Large, dark-reddish, needle-like single crystals suitable for X-ray crystallography were obtained after several weeks (ca. 75% yield). ^{1}H NMR (22 °C, benzene-d_6): δ 0.360 (s, broad, CH_3). ^{13}C NMR (benzene-d_6): δ 3.142 (CH_3).

Structure Determination. X-ray diffraction data sets of single crystals of the compounds were collected at 120 K on either Bruker D8 APEX-II or Bruker X8 APEX-II diffractometers equipped with CCD area detectors using graphite-monochromated Mo Kα radiation. The single crystals were selected under Paratone-N oil, mounted on Mitegen micromount loops, and positioned in the cold stream of the diffractometer. The structures were solved by direct methods and refined on F^2 using the SHELXTL V6.21 package. Further details of the data collections and refinements are listed in Table 1.

Table 1. Selected Data Collection and Refinement Parameters for Compounds 1−3

compound	1	2	3
formula weight	1425.36	1686.78	1600.68
space group, Z	$P2_1/n$, 8	$R\bar{3}$, 42	$P\bar{1}$, 4
a (Å)	23.163(5)	64.496(14)	9.4878(13)
b (Å)	23.872(5)	64.496(14)	23.854(3)
c (Å)	23.166(5)	22.031(5)	28.076(4)
α (deg)	90	90	88.995(3)
β (deg)	99.96(3)	90	83.354(3)
γ (deg)	90	120	87.937(3)
V (Å^3)	12617(5)	79366(29)	6307.0(15)
radiation, λ (Å)		Mo Kα, 0.71073	
ρ_{calcd} (g·cm^{-3})	1.501	1.482	1.686
μ (mm^{-1})	4.472	4.062	7.014
$R1/wR2$,[a] $I \geq 2\sigma_I$	0.0350, 0.0699	0.1028, 0.2420[b]	0.0348, 0.0781
$R1/wR2$,[a] all data	0.0571, 0.0793	0.2022, 0.2883[b]	0.0490, 0.0898

[a] $R1 = [\Sigma||F_0| - |F_0||]/\Sigma|F_0|$; $wR2 = \{[\Sigma w[(F_0)^2 - (F_c)^2]^2]/[\Sigma w(F_0^2)^2)]\}^{1/2}$; $w = [\sigma^2(F_0)^2 + (AP)^2 + BP]^{-1}$, where $P = [(F_0)^2 + 2(F_c)^2]/3$. Mo K$\alpha$, 0.71073. [b] The relatively large R values for compound **2** are due to the extremely large unit cell (~80 000 Å^3) with three crystallographically different molecules.

NMR Spectroscopy. Deuterated benzene (Cambridge Isotope Laboratories, 99.9%) and deuterated toluene (Cambridge Isotope Laboratories, 99.9%) were used as solvents. ^{1}H, ^{13}C, and ^{29}Si NMR spectra were recorded on a Varian INOVA 500 MHz spectrometer locked on the deuterium solvent and referenced against Me_4Si (tetramethylsilane, Sigma-Aldrich, 99.9+%).

Variable-Temperature NMR Spectroscopy. ^{1}H NMR spectra of **1** and **3** were recorded on a Varian VXR-500 NMR spectrometer in the temperature ranges from −60 to +100 °C in toluene-d_8 and −80 to +60 °C in THF-d_8. The data were processed using the program gNMR to generate calculated line shapes and to superimpose them on the observed spectra in order to derive the rate constants for the processes.[19] Activation parameters were calculated by plotting $\ln(k_m/T)$ versus $1/T$.

Mass Spectrometry. Electrospray mass spectra (ES-MS) were recorded in negative-ion mode on a Micromass Quattro-LC triple quadrupole mass spectrometer (typical conditions: 125 °C source temperature, 150 °C desolvation temperature, 2.8 kV capillary voltage, 30−80 V cone voltage). The samples were introduced by direct infusion with a Harvard syringe pump at 10 μL/min. The samples were taken from the corresponding reaction mixtures just before setting them aside for crystallization.

RESULTS AND DISCUSSION

Synthesis. Clearly, the nature of the solvent for the reaction of K_4Ge_9 with RX plays a major role in "determining" the maximum number of substituents that attach to the Ge_9 deltahedral clusters. At this stage, it is not clear whether the most important factor is the polarity of the solvent, its dielectric constant, its basicity, its coordinating ability, the relative solubility of the differently substituted clusters, a combination of these, or yet possibly something else. Obviously more data points are needed for a more general conclusion. What is known at this stage is that treating a suspension of K_4Ge_9 precursor in MeCN or THF with $(Me_3Si)_3SiCl$ generates almost exclusively the trisubstituted monoanions $[Ge_9\{Si-$

dx.doi.org/10.1021/ja505826x | J. Am. Chem. Soc. 2014, 136, 12056−12063

Scheme 1. Bonding Modes for a Substituent *exo*-Bonded to a Ge_9 Cluster[a]

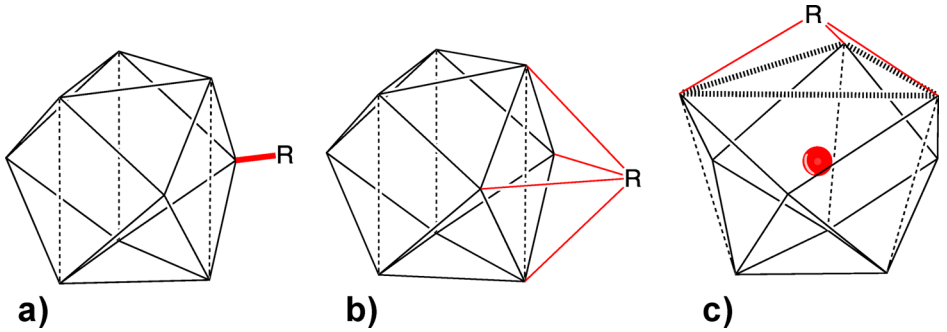

[a](a) The substituent is bonded to one vertex by a normal 2-center−2-electron *exo*-bond; (b) the substituent caps one of the three possible pseudosquare faces to form a bicapped square antiprism; (c) the substituent caps one of the triangular bases of the tricapped trigonal prismatic cluster $M@Ge_9$ centered by a metal atom (M shown in red) and pushes that base open.

$(SiMe_3)_3\}_3]^-$ while the mono- and disubstituted species are present only as traces according to the mass spectra of the reaction mixtures. Also, according to NMR of the latter, tetra-hypersilylated neutral molecules do not form either. At the same time, the analogous reaction carried out in DMF suspension of the precursor produces almost exclusively the disubstituted species with traces of the monosubstituted clusters but not even a hint of trisubstitution. It should be mentioned that the reaction cannot be carried out in ethylenediamine simply because the silyl chloride reacts with the solvent. Also, no detectable reaction occurs in highly nonpolar solvents such as toluene and hexane.

The ability to synthesize the tri-hypersilylated monoanionic clusters $[Ge_9R_3]^-$ (R = $-Si(SiMe_3)_3$) in large amounts by the approach described above makes them convenient and readily available starting species for follow-up reactions. Its over-saturated solution/suspension in benzene was used originally for the synthesis of the first tetrasubstituted clusters $[Ge_9\{Si(SiMe_3)_3\}_3\{SnPh_3\}]$ (**4**) by a reaction with Ph_3SnCl.[12] This same approach was also used for the synthesis of the reported compounds **2** and **3** as products of the reactions with $^nBu_3SnCl$ and TlCp, respectively. The synthesis of **1**, on the other hand, was carried out in acetonitrile, which is known to favor strongly S_N2 reactions. The successful synthesis with the primary bromide EtBr and the observed fast reaction supports that mechanism. Furthermore, as expected for the S_N2 mechanism, the reaction with a secondary bromide such as ^{i}PrBr was observed to be much slower. Also, the reactions with alkyl iodides such as MeI and ^{i}PrI were significantly faster than the corresponding bromides, while those with alkyl chlorides were almost undetectable. Lastly, no reaction was observed with tertiary bromides such as ^{t}BuBr. Similarly, no reactions were observed in nonpolar solvents such as benzene and toluene, independent of the nature of the alkyl bromide. Overall, the neutral tetrasubstituted species are soluble in very nonpolar solvents such as benzene, toluene, pentane, and hexane, while the trisubstituted monoanions, $(Ge_9R_3)^-$, are soluble in fairly polar solvents such as THF, MeCN, and DMF.

Structures. The naked nine-atom germanium cores, Ge_9^{4-}, are deltahedral *nido*-clusters that follow the Wade−Mingos electron-counting rules developed for boranes with $2n + 4 = 22$ ($n = 9$ vertices) cluster-bonding electrons and $2n = 18$ external electrons (lone pairs in this case; one per vertex), totalling 40 cluster valence electrons.[20] The geometry, often viewed as a monocapped square antiprism, is better and more generally described as a tricapped trigonal prism with one, two, or three elongated prismatic edges parallel to the three-fold axis. (The monocapped square antiprism is one specific case of a tricapped trigonal prism with one such edge elongated to a specific length.) Upon functionalization, the substituent takes one of two different positions at the cluster depending on the nature of the substituent. Electron-rich main-group fragments such as R_3E (E = C, Si, Ge, Sn) and R_2E (E = Sb, Bi) form *exo*-bonds with one of the three prism-capping Ge atoms (Scheme 1a).[2−5] The latter are only four-connected within the cluster and, thus, more susceptible to form *exo*-bonds than the remaining six prism-forming atoms which are five-connected. Electron-poor cluster substituents, on the other hand, cap one of the three pseudosquare faces of the tricapped trigonal prism (each face is made of a pair of capping and a pair of prismatic atoms and contains an elongated edge), thus forming a *closo*-cluster with the expected shape of a bicapped square antiprism (Scheme 1b). Such substituents are typically ligated transition-metal atoms that "need" the six electrons provided by the square face.[1,21−26] Similarly, a single thallium atom takes the same position where it uses two of its three electrons for an external lone pair and contributes its third electron to the cluster-bonding pool, thus reducing the charge of the cluster by one, that is, $[Ge_9Tl]^{3-}$.[27] Lastly, the same Ge_9 clusters but with an interstitial central atom, that is, endohedral clusters $M@Ge_9^{n-}$, can also be functionalized with ligated transition-metal atoms but yet at a different position on the cluster. In this case, the substituent caps one of the triangular bases of the tricapped trigonal prism and is "pulled" by the central atom to form pseudospherical species, thus causing expansion of the capped triangular base to nearly nonbonding distances (Scheme 1c).[28,29]

The addition of three hypersilyl groups to Ge_9^{4-} follows the expected pattern for electron-rich substituents; that is, they bond to the three capping Ge atoms as they are the only four-connected vertices in the cluster. The resulting trisubstituted $[Ge_9\{Si(SiMe_3)_3\}_3]^-$ is again a tricapped trigonal prism, and this time, all three prismatic edges are elongated equally along the three-fold axis (Scheme 2). This shape with its six equivalent naked Ge atoms offers fairly limited bonding modes for a fourth substituent to produce a neutral molecule. The choices are (i) a normal 2-center−2-electron radially pointing *exo*-bond at one Ge atom (analogous to Scheme 1a); (ii) a multicenter 2-electron *exo*-bond involving two or three Ge atoms at one triangular base (discussed for compound **2** below); (iii) capping and expanding one of the two available triangular bases of the trigonal prism (the same as that in a

dx.doi.org/10.1021/ja505826x | J. Am. Chem. Soc. 2014, 136, 12056−12063

Scheme 2. Trisubstituted Clusters $[Ge_9\{Si(SiMe_3)_3\}_3]^-$ with a D_{3h} Symmetry[a]

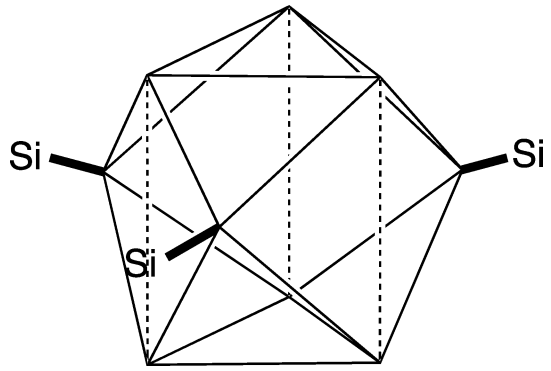

[a]Only the *exo*-bonded Si atoms of the hypersilyl groups are shown.

centered naked cluster; Scheme 1c); (iv) capping one of the three available pseudosquare faces made of two capping and two prismatic Ge atoms (the same as that in the naked cluster; Scheme 1b). Schnepf et al. have reported examples of mode (iii),[16−18] while mode (ii) was reported by us in the neutral $[Ge_9\{Si(SiMe_3)_3\}_3\{SnPh_3\}]$ (**4**).[12] The fourth substituent $SnPh_3$ in the latter *exo*-bonds to one Ge atom, but the bond is not radial to the cluster. Instead, it is tilted toward the other two Ge atoms of the base, which suggests some nonzero interactions of these Ge atoms with the substituent. Compounds **1** and **3** reported here exhibit the remaining two modes, (i) and (iv), respectively, while compound **2** contains three crystallographically different clusters with three different positions for the fourth substituent that are somewhere between modes (i) and (ii).

Compound **1**, $Ge_9[Si(SiMe_3)]_3(CH_2CH_3)$, is the first tetrasubstituted species with an organic substituent, an ethyl group in this case. The structure contains two crystallographically unique but almost identical molecules **1a** and **1b** with only minor differences in the conformation of the ethyl group. The latter is *exo*-bonded to one prismatic Ge atom by a normal 2-center−2-electron Ge−C bond that points radially away from the cluster core (Figure 1). The two Ge−C distances, virtually identical at 1.973(4) and 1.975(4) Å, compare well with 2.007(5) Å in $[^tBu-Ge_9-Ge_9-^tBu]^{4-}$ with tertiary carbon atoms and with the statistical mean distance of 1.965 Å derived from more than 500 distances between sp^3-hybridized Ge and C atoms listed in the Cambridge Structural Database.[5,30] As it has been observed before, the distances within the Ge_9 cluster core are also affected by the additional substituent.[1] Typically, an *exo*-bond to a cluster atom causes elongation of a cluster edge (or edges) to this atom that is (are) opposite or nearly opposite to the *exo*-bond. This is exactly the case in **1** where the trigonal prismatic edge parallel to the pseudo-three-fold axis at the *exo*-bonded Ge atom is elongated to 3.650(9) Å in **1a** compared to the other two edges of 3.055(8) and 3.069(8) Å. (The numbers are very similar in **1b**.)

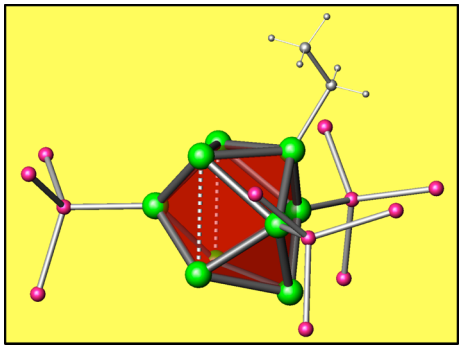

Figure 1. Tetrasubstituted clusters $Ge_9\{Si(SiMe_3)_3\}_3Et$ of compound **1** (Ge, green; Si, purple; C and H, gray; the methyl groups bonded to Si are not shown).

Compound **2**, $[Ge_9\{Si(SiMe_3)_3\}_3\{Sn^nBu)_3\}]$, contains three crystallographically different clusters **2a**, **2b**, and **2c** (Figure 2).

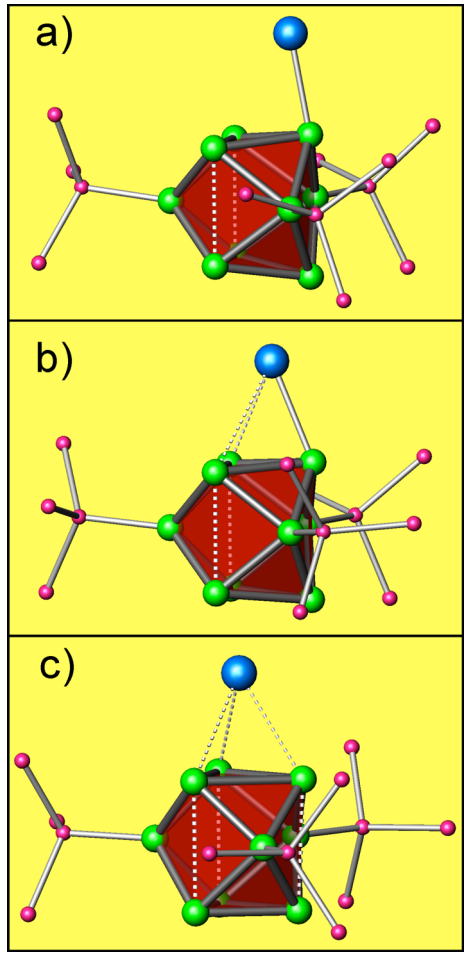

Figure 2. Three different clusters $Ge_9\{Si(SiMe_3)_3\}_3\{Sn^nBu)_3\}$ in the structure of compound **2** with the Sn atom bonded to (a) predominantly one Ge vertex, (b) one Ge vertex but also interacting substantially with the other two vertices in the triangular base, and (c) all three Ge vertices of the triangular base equally (Ge, green; Si, purple; Sn, blue; the methyl groups bonded to Si and the *n*-butyl groups bonded to Sn are not shown).

However, unlike the virtually identical **1a** and **1b** in compound **1**, these three clusters differ noticeably in the bonding modes of the fourth substituent Sn^nBu_3. Thus, the latter in **2a** is bonded almost exclusively to one of the prismatic Ge atoms (Figure 2a) with a Ge−Sn distance of 2.685(2) Å that compares well with those in $[Ge_9-SnMe_3]^{3-}$, $[Ph_3Sn-Ge_9-SnPh_3]^{2-}$, and $[Ph_3Sn-Ge_9-Ge_9-SnPh_3]^{4-}$ of 2.695(1), 2.617(1), and 2.650(2) Å, respectively.[2] However, unlike the radially positioned Ge−C bond in **1**, the Ge−Sn bond is slightly tilted toward the neighboring trigonal prismatic base with Ge−Sn distances to

dx.doi.org/10.1021/ja505826x | J. Am. Chem. Soc. 2014, 136, 12056−12063

the other two Ge atoms of 3.625(2) and 3.725(2) Å that are not completely nonbonding. Nonetheless, as in **2a**, the Ge−Sn *exo*-bond leads to similar elongation of the vertical prismatic edge associated with the *exo*-bonded Ge-atom, namely, 3.666(3) Å compared to the other two edges of 3.058(3) and 3.042(3) Å (Figure 2a).

In **2b**, the Ge−Sn *exo*-bond is tilted significantly more toward the same trigonal prismatic base positioning the Sn atom closer to the pseudo-three-fold axis (Figure 2b). This leads to shortening of the distances to the two opposite Ge atoms, 3.407(3) and 3.313(3) Å, and lengthening of the one to the Ge atom to which it is primarily bonded, 2.802(3) Å. This, in turn, results in elongations of all three vertical prismatic edges of the Ge_9 core. The degree of elongation is inversely proportional to the corresponding Ge−Sn distance, namely, 3.108(2), 3.185(2), and 3.534(3) Å Ge−Ge distances corresponding to the longest, medium, and shortest Ge−Sn distances, respectively.

Lastly, the tin atom in **2c** is positioned exactly on the three-fold axis of the cluster, which, in turn, is positioned on the three-fold axis of the unit cell and has perfect C_{3v} point-group symmetry (Figure 2c). The three equal Ge−Sn distances are 3.092(4) Å, and the three corresponding prismatic Ge−Ge edges are elongated at 3.284(4) Å.

The three different positions of the fourth substituent in **2a**, **2b**, and **2c** suggest dynamic behavior of the substituent in solution. Apparently, the crystal structure has captured three "frozen" snapshots of these dynamics. All of this is in excellent agreement with the ^{1}H and ^{13}C NMR spectra measured at room temperature, which show only one hypersilyl signal. This, in turn, is consistent with the Sn^{n}Bu$_3$ substituent either moving between the germanium atoms at a rate faster than the NMR time scale or simply staying at the three-fold axis while in solution and only shifting off of it upon crystallization due to packing requirements. Cooling the solution all the way down to −90 °C does not change the situation; that is, only small peak broadening is observed but with no indication for separation (discussed more below).

The geometry of $Ge_9Tl\{Si(SiMe_3)_3\}_3$ (**3**) is different than all other tetrasubstituted Ge_9 clusters. Here the Tl atom is found between two hypersilyl groups capping the pseudosquare face made of two *exo*-bonded and two prismatic germanium atoms (Figure 3). This is exactly the same position that thallium takes when added to naked Ge_9 clusters to form the 10-atom *closo*-$[Ge_9Tl]^{3-}$ (a bicapped square antiprism).[27] In this respect, the new species $Ge_9Tl\{Si(SiMe_3)_3\}_3$ can be viewed as $[Ge_9Tl]^{3-}$ that is trisubstituted with hypersilyl groups to give its neutrality. The crystal structure of **3** contains again two crystallographically different but otherwise nearly identical $Ge_9Tl\{Si(SiMe_3)_3\}_3$ clusters **3a** and **3b**. Focusing on just one of them, we see that the Tl atom takes one of the two capping positions in the bicapped square antiprism $[Ge_9Tl]^{3-}$ with Ge−Tl distances in the range of 3.0676(6)−3.1015(6) Å. These distances are noticeably longer than the range of 2.9049(5)−2.9969(6) Å observed in the naked $[Ge_9Tl]^{3-}$ cluster.[25] In addition, the germanium square capped by thallium is significantly smaller in **3** than in $[Ge_9Tl]^{3-}$ with ranges of Ge−Ge distances of 2.6261(8)−2.6488(7) Å in the former and 2.6971(7)−2.7300(7) Å in the latter. Both observations suggest that the thallium atom in **3** participates much less in the bonding of the cluster than it does in $[Ge_9Tl]^{3-}$; that is, it interacts more strongly with the cluster in the latter. This is confirmed by NMR spectroscopy, which suggests dissociation−association dynamic behavior of the thallium vertex (discussed in detail below).

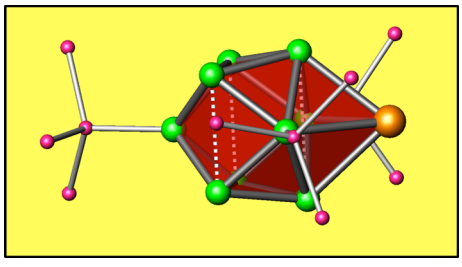

Figure 3. Structure of tetrasubstituted clusters $Ge_9\{Si(SiMe_3)_3\}_3Tl$ (**3**) (Ge, green; Si, purple; Tl, orange; the methyl groups bonded to Si are not shown).

Solution Studies. According to the ^{1}H NMR spectra collected at room temperature in THF-d_8, all three compounds exhibit dynamic behavior. More specifically, the three silyl groups behave as equivalent and produce a single proton peak that is fairly sharp for **2** but significantly broadened for **1** and **3**. For compound **2** as well as for the previously reported compound **4**, this situation does not change upon cooling to −90 °C. Such behavior is consistent with a dynamic SnR_3 substituent moving very fast between the three Ge atoms of one of the prismatic faces. This is very strongly supported by the crystal structures of both **2** and **4**, which exhibit clusters where the fourth substituent is found at slightly different positions above the triangular prismatic base. The differences are most likely due to packing requirements and are consistent with a very labile SnR_3 substituent. The same dynamics has been observed also for Sn_9 clusters monosubstituted with a similar organo−tin fragment, namely, $[Sn_9–SnCy_3]^{3-}$, where Cy = cyclohexane.[31] Eichhorn et al. reported that the ^{119}Sn NMR spectrum of the compound broadened when cooled to −55 °C, but a limiting spectrum was not observed. By examining the ^{119}Sn−^{119}Sn and ^{117}Sn−^{119}Sn couplings between the cluster and substituent Sn atoms, the authors concluded that the substituent rapidly scrambles around the outside of the Sn_9 cluster.[32]

The dynamics of compound **3** is of different nature. To begin with, the room temperature ^{1}H NMR spectrum in toluene-d_8 shows two broad peaks for the hypersilyl protons in a ratio of 2:1. Furthermore, upon cooling (stepwise to −60 °C), the peaks become sharper and move further apart (Figure 4). At the same time, upon heating to 100 °C (stepwise), the two peaks initially become even broader and move closer to each other, then they merge into one broad peak at about 70 °C, and that peak becomes sharper at higher temperatures. All of this is consistent with classical temperature dependence of the rate of a reaction with reasonable parameters to allow for observation in a practical range of temperatures. Following the observed lability of the SnR_3 substituents in **2** and **4**, it was similarly proposed that the thallium atom in **3** moves between the three equivalent pseudosquare faces of $[Ge_9\{Si(SiMe_3)\}]^-$. The spectra were analyzed quantitatively in order to extract the rate constants at each temperature. The Eyring plot (Figure S1 in Supporting Information) of the temperature dependence of these rate constants provided the thermodynamic parameters for the transition state: $\Delta H^{\ddagger}$ = 48.9 ± 1.4 kJ·mol^{-1}, $\Delta S^{\ddagger}$ = −50.4 ± 1.4 J·mol^{-1}·K^{-1}, and $\Delta G_{298}{}^{\ddagger}$ = 63.9 ± 1.9 kJ·mol^{-1}. At this point, it was important to try to find more information on the nature of the dynamic process, that is, whether the thallium

dx.doi.org/10.1021/ja505826x | J. Am. Chem. Soc. 2014, 136, 12056−12063

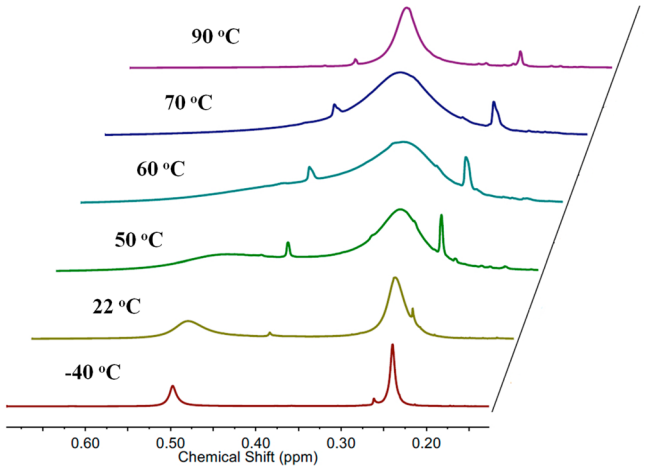

Figure 4. Variable-temperature ^{1}H NMR spectra of compound **3** in toluene-d_8.

migration is intramolecular, with the thallium atom moving from a face to face without separating from the cluster, or the process involves dissociation of the thallium cation as solvated species followed by association at the same or another face of the cluster. Since the dissociation process would depend on the coordinating capabilities of the solvent, the expectation is that the intermolecular reaction rates in differently coordinating solvents would differ substantially. Thus, variable-temperature ^{1}H NMR measurements (−80 to +60 °C) were carried out on compound **3** dissolved in THF-d_8 (Supporting Information Figure S2) instead of toluene-d_8. Unlike the two broad peaks observed at room temperature in toluene-d_8, the spectrum in THF shows a single broad peak, and this indicates significantly higher reaction rate of the dynamic process in this solvent. Indeed, the two rate constants, k_{298}, extracted after analysis of the spectra are in a ratio of 60:8000 s^{-1}; that is, the reaction rate in THF is more than 130 times higher than that in toluene (Figure S3). The corresponding thermodynamic parameters for the transition state in THF are $\Delta H^{\ddagger}$ = 41.5 ± 2.5 kJ·mol^{-1}, $\Delta S^{\ddagger}$ = −34.3 ± 1.9 J·mol^{-1}·K^{-1}, and $\Delta G_{298}{}^{\ddagger}$ = 51.7 ± 3.1 kJ·mol^{-1}. The different rates and free energies suggest that the solvent plays an important role in the reaction mechanism. Thus, it is very likely that compound **3** undergoes dissociation to $[Ge_9\{Si(SiMe_3)_3\}_3]^-$ and Tl^+ that is accompanied by solvation of the ions and following association of the Tl^+ back to a pseudosquare face. As THF is a more polar and basic solvent than toluene, Tl^+ is solvated much better by it, which in turn stabilizes better the transition state (lower energy barrier) and increases the reaction rate. All of these observations indicate that, as expected, compound **3** is considerably ionic and can be viewed as made of a thallium cation and a trisubstituted cluster anion.

Compound **1** with its strong and radially positioned 2-center−2-electron Ge−C *exo*-bond was expected to be static in solution (i.e., without dynamic processes). To our surprise, however, its room temperature ^{1}H NMR spectrum in deuterated toluene showed one broad peak for the hypersilyl protons while the protons of the ethyl substituent appeared sharp and normal. Upon cooling, similar to compound **3**, the hypersilyl proton peak broadened further, then split into two broad peaks in a 2:1 ratio, and finally, the peaks became sharper and separated further (Figure S4). Also, upon heating above room temperature, the single peak became sharper. Clearly, some type of dynamic process occurs in solution for this compound, as well. However, it is difficult to imagine that this would occur via either dissociation/association of the ethyl group (impossible process) similar to the thallium substituent in compound **3** or by an intramolecular "walk" of the ethyl group moving over the Ge atoms of the trigonal prismatic base similar to the SnR_3 substituents in compounds **2** and **4**. Nonetheless, in order to rule out the former as well as dissociation by the hypersilyl groups, we carried out variable-temperature ^{1}H NMR measurements also in deuterated THF (Figure S5). The derived free energies for the two solvents, $\Delta G_{298}{}^{\ddagger}$ = 57.7 ± 2.3 kJ·mol^{-1} ($\Delta H^{\ddagger}$ = 63.5 ± 2.5 kJ·mol^{-1}; $\Delta S^{\ddagger}$ = 19.4 ± 0.8 J·mol^{-1}·K^{-1}) in toluene and $\Delta G_{298}{}^{\ddagger}$ = 59.0 ± 2.6 kJ·mol^{-1} ($\Delta H^{\ddagger}$ = 45.2 ± 2.0 kJ·mol^{-1}; $\Delta S^{\ddagger}$ = −46.4 ± 2.3 J·mol^{-1}·K^{-1}) in THF, are virtually identical and so are the corresponding rate constants which are in a ratio of 1.1:1 (Figure S6). This clearly indicates that the process is mostly solvent-independent and, thus, unlikely to involve dissociation of a substituent.

Intramolecular scrambling of the ethyl group is also easily ruled out based on previous studies of the dynamics of Sn_9 clusters functionalized with an isopropyl group, $[Sn_9(i\text{-}Pr)]^{3-}$.[31] On the basis of the observed ^{119}Sn and ^{117}Sn NMR spectra and their coupling patterns, the authors concluded that the Sn−C bond is nonlabile. Rather, the substituent travels together with the tin atom to which it is *exo*-bonded by a mechanism where the whole cluster is fluxional, exchanging the positions of all nine atoms. Unfortunately, there is no NMR-suitable germanium nucleus (the only spin-active isotope is quadrupolar), and similar direct observations of the mechanism of the dynamics in substituted Ge_9 clusters are impossible. Nonetheless, on the basis of the results for Sn−C, we can safely assume that the stronger Ge−C bond is also nonlabile.

The indirect observations of the dynamics in $Ge_9\{Si(SiMe_3)_3\}_3Et$ by ^{1}H NMR presented above are consistent with two possible scenarios depending on whether the Ge−Si bonds are labile or not. In the first one, the nine Ge atoms scramble among their different positions with the substituents "riding" on four of them; that is, the Ge_9 core is fluid like its tin analogue, independent of the fact that it has four substituents attached to it.[31−35] This scenario assumes that not only the Ge−C but also the three Ge−Si bonds are nonlabile. Using a ball-and-stick magnetic model kit, we tried very extensively to envision possible stepwise mechanisms in which the Ge−Et fragment would travel around the trigonal prismatic base. All we could find, however, were multistep processes involving a minimum of six bond-breaking and six bond-forming acts. Furthermore, most of the intermediate geometries of the cluster are extremely unlikely in terms of both impossible connectivities and large deviations from a spherical shape. Nonetheless, this scenario should be considered possible because it is consistent with a similar observation for the hypersilyl-substituted tin cluster $Sn_{10}\{Si(SiMe_3)_3\}_6$.[36] In that case, the ^{1}H NMR spectrum shows a single peak at room temperature despite the fact that the six substituents are *exo*-bonded to tin atoms with three structurally different environments according to the solid-state structure. This would suggest that the tin atoms scramble among the different positions carrying with them the substituents.

The second possible scenario for the observed dynamics in **1** assumes labile Ge−Si bonds and, thus, dynamic behavior of the cluster core as detached from the hypersilyl substituents (but with attached ethyl group). A very strong argument in favor of

dx.doi.org/10.1021/ja505826x | J. Am. Chem. Soc. 2014, 136, 12056−12063

this scenario is that energetically the Ge−Si bond is by far closer to the labile Ge−Sn bond than it is to the nonlabile Ge−C bond. For example, the bond dissociation energies of the corresponding diatomic molecules are 297 kJ/mol for Ge−Si, 230 kJ/mol for Ge−Sn, and 456 kJ/mol for Ge−C.[37] The simplest possible movement of the detached Ge_9Et core would be rotation around its pseudo-three-fold axis. Such rotation would take the hypersilyl groups from their radial *exo*-bonded positions to positions that bridge pairs of germanium atoms, as shown in Scheme 3. It would explain very well the observed temperature dependence of the proton NMR. At this stage, however, it is impossible to distinguish between the two mechanisms.

Scheme 3. Proposed Transition State for the Rotation of the Ge_9Et Core around Its Pseudo-Three-Fold Axis (Vertical) in Which the Hypersilyl Groups Bridge Pairs of Vertices

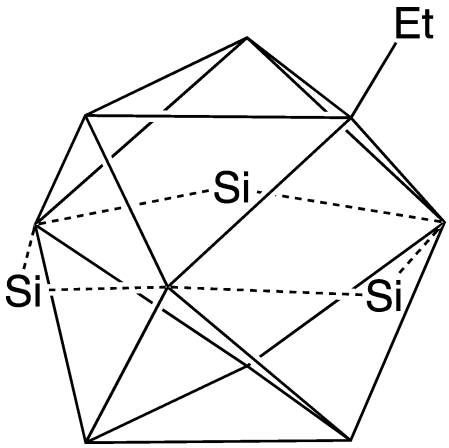

Independent of which mechanism takes place in the cluster dynamics of compound **1**, it is logical to assume that the same dynamic process occurs for compounds **2** and **3**. However, it is most likely masked in the latter two compounds by the much faster process of the SnR_3 substituent hopping between three vertices in **2** and by the thallium dissociation−association process in **3**. These studies clearly show that the tetrasubstituted nine-atom germanium clusters are fluxional, perhaps similar to their naked and monosubstituted tin analogues, an observation which could not be made before for the naked or less-substituted clusters due to the lack of appropriate for NMR germanium isotopes or the high symmetry of the substituted species.

■ ASSOCIATED CONTENT

Supporting Information

X-ray crystallographic file in CIF format and variable-temperature ^{1}H NMR spectra. This material is available free of charge via the Internet at http://pubs.acs.org.

■ AUTHOR INFORMATION

Corresponding Author

ssevov@nd.edu

Notes

The authors declare no competing financial interest.

■ ACKNOWLEDGMENTS

We thank the National Science Foundation (CHE-0742365) for the financial support of this research, and Prof. Seth Brown for his help with processing and interpretation of the variable-temperature NMR data.

■ REFERENCES

(1) For recent reviews, see: (a) Scharfe, S.; Kraus, F.; Stegmaier, S.; Schier, A.; Fässler, T. F. *Angew. Chem., Int. Ed.* **2011**, *50*, 3630. (b) Fässler, T. F. *Struct. Bonding* **2011**, *140*, 91. (c) Sevov, S. C.; Goicoechea, J. M. *Organometallics* **2006**, *25*, 5678. (d) Fässler, T. F. *Coord. Chem. Rev.* **2001**, *215*, 347.
(2) Ugrinov, A.; Sevov, S. C. *Chem.—Eur. J.* **2004**, *10*, 3727.
(3) Ugrinov, A.; Sevov, S. C. *J. Am. Chem. Soc.* **2003**, *125*, 14059.
(4) Ugrinov, A.; Sevov, S. C. *J. Am. Chem. Soc.* **2002**, *124*, 2442.
(5) Hull, M. W.; Ugrinov, A.; Petrov, I.; Sevov, S. C. *Inorg. Chem.* **2007**, *46*, 2704.
(6) Hansen, D. F.; Zhou, B.; Goicoechea, J. M. *J. Organomet. Chem.* **2012**, *721−722*, 53.
(7) Benda, C. B.; Wang, J. Q.; Wahl, B.; Fässler, T. F. *Eur. J. Inorg. Chem.* **2011**, 4262.
(8) Hull, M. W.; Sevov, S. C. *Angew. Chem., Int. Ed.* **2007**, *46*, 6695.
(9) Hull, M. W.; Sevov, S. C. *Inorg. Chem.* **2007**, *46*, 10953.
(10) Hull, M. W.; Sevov, S. C. *J. Am. Chem. Soc.* **2009**, *131*, 9026.
(11) Li, F.; Sevov, S. C. *Inorg. Chem.* **2012**, *51*, 2706.
(12) Li, F.; Muñoz-Castro, A.; Sevov, S. C. *Angew. Chem., Int. Ed.* **2012**, *51*, 8581.
(13) Schnepf, A. *Angew. Chem., Int. Ed.* **2003**, *42*, 2624.
(14) Schenk, C.; Schnepf, A. *Chem. Commun.* **2009**, 3208.
(15) Henke, F.; Schenk, C.; Schnepf, A. *Dalton Trans.* **2011**, *40*, 6704.
(16) Schenk, C.; Schnepf, A. *Angew. Chem., Int. Ed.* **2007**, *46*, 5314.
(17) Schenk, C.; Henke, F.; Santiso-Quiñones, G.; Krossing, I.; Schnepf, A. *Dalton Trans.* **2008**, *33*, 4436.
(18) Henke, F.; Schenk, C.; Schnepf, A. *Dalton Trans.* **2009**, 9141.
(19) Budzelaar, P. H. M. *gNMR*, v.3.6.5; Cherwell Scientific Publishing: Oxford, 1996.
(20) Wade, K. J. *Adv. Inorg. Chem. Radiochem.* **1976**, *18*, 1.
(21) Eichhorn, B. W.; Haushalter, R. C.; Pennington, W. T. *J. Am. Chem. Soc.* **1988**, *110*, 8704.
(22) Kesanli, B.; Fettinger, J. C.; Eichhorn, B. W. *Chem.—Eur. J.* **2001**, *7*, 5277.
(23) Eichhorn, B. W.; Haushalter, R. C. *Chem. Commun.* **1990**, 937.
(24) Campbell, J.; Mercier, H. P. A.; Holger, F.; Santry, D.; Dixon, D. A.; Schrobilgen, G. J. *Inorg. Chem.* **2002**, *41*, 86.
(25) Yong, L.; Hoffmann, S. D.; Fässler, T. F. *Eur. J. Inorg. Chem.* **2005**, 3663.
(26) Goicoechea, J. M.; Sevov, S. C. *Organometallics* **2006**, *25*, 4530.
(27) Rios, D.; Gillett-Kunnath, M. M.; Taylor, J. D.; Oliver, A. G.; Sevov, S. C. *Inorg. Chem.* **2011**, *50*, 2373.
(28) Goicoechea, J. M.; Sevov, S. C. *Angew. Chem., Int. Ed.* **2005**, *44*, 4026.
(29) Goicoechea, J. M.; Sevov, S. C. *J. Am. Chem. Soc.* **2006**, *128*, 4155.
(30) Allen, F. H. *Acta Crystallogr.* **2002**, *B58*, 380.
(31) Kocak, S.; Zavalij, P.; Lam, Y.-F.; Eichhorn, B. *Chem. Commun.* **2009**, 4197.
(32) Eichhorn, B. W.; Kocak, F. S. *Struct. Bonding* **2011**, *140*, 59.
(33) Kesanli, B.; Halsig, J. E.; Zavalij, P.; Fettinger, J. C.; Lam, Y.-F.; Eichhorn, B. W. *J. Am. Chem. Soc.* **2007**, *129*, 4567.
(34) Kocak, F. S.; Zavalij, P.; Lam, Y.-F.; Eichhorn, B. W. *Inorg. Chem.* **2008**, *47*, 3515.
(35) Esenturk, E. N.; Fettinger, J. C.; Eichhorn, B. W. *J. Am. Chem. Soc.* **2006**, *128*, 12.
(36) Schrenk, C.; Schellenberg, I.; Pöttgen, R.; Schnepf, A. *Dalton Trans.* **2010**, *39*, 1872.

(37) Luo, Y. Bond Dissociation Energies. *CRC Handbook of Chemistry and Physics*; CRC Press: Boca Raton, FL, 2010; section 9, p 65.